MODELLING AND NUMERICAL SIMULATIONS OF A TB51 ROAD CRASH TEST USING A SIMPLIFIED COACH MODEL

PAWEŁ DZIEWULSKI[1]

Military University of Technology

Summary

The paper proposes a methodology of a TB51 virtual crash test on the example of the selected bridge protective barrier, using a simplified coach model. In simulations of crash tests, the non-linear, explicit finite element code LS-Dyna v971 was used. The simulation results corresponding to the simplified model were compared with the simulation results for a quasi-accurate model and the experimental crash test results. It was shown that the simplified vehicle model can be used in tests certifying a barrier modified in relation to the certified reference barrier.

Keywords: bridge protective barrier, TB51 crash test, methodology of numerical modelling, numerical validation, experimental validation

1. Foreword

Certification tests of road and bridge protective barriers are executed in accordance with European standards [4, 5]. These standards include the collection of the information necessary to execute experimental field tests of selected traffic safety equipment. With the introduction of the standard [17], certification of barriers modified with the help of numerical simulations or other calculations became possible. The standard [17] gives the requirements for conformity assessment for road barriers and other vehicle restraint systems, but does not specify how to execute the numerical simulation or other calculations of a modified system.

Modelling and experimental verification of road crash test is subject to a series of publications. The paper [9] considers a straight road barrier with an A-type guide bar, in which easily deformable spacers connecting the guide bar with posts were used. The modelling assumes that the guide bar is a continuous beam. The elastic-plastic model of

[1]   Military University of Technology, Faculty of Mechanical Engineering, Department of Mechanics and Applied Computer Science, ul. Kaliskiego 2, 00-908 Warsaw; e-mail: pdziewulski@wat.edu.pl

steel was adopted. In order to validate the modelling, numerical results (ASI index, working width) corresponding to the TB11 test were compared with experimental results.

In the paper [3], among others, FEM numerical modelling and simulations of the TB11 crash test with respect to the straight section (36.00 m) of an SP-05/4 road barrier (bars at 4.00 m, manufacturer Stalprodukt S.A., Bochnia), without or with an energy-consuming crash barrier, were conducted. The numerical model of the Suzuki Swift vehicle was downloaded from the NCAC public library [10]. The steel-foam, energy-consuming crash barrier with a trapezoidal cross-section, which is connected to a B-type guide bar along the top and bottom edge by riveting, was used. It was assumed that the posts are fixed in a rigid substrate. The effect of the density of the barrier's foam filling on energy absorbed by the barrier and change of the speed of the car's centre of gravity was examined.

In the paper [8], experimental and numerical tests of a transverse impact of the Suzuki Swift car at a speed of 45.5 km/h at the SP-04/2 barrier section without and with the composite-foam crash barrier were conducted. The crash barrier consists of a glass-polyester composite (one layer of fabric with straight interlace, grammage of 450g/m^2) with a trapezoidal profile and polyurethane foam filling. The guide bar is attached to the IPE140 posts. The posts were fixed in a concrete slab. Time courses of acceleration of the centre of vehicle mass, the vehicle and barrier's deformations and the barrier's energy consumption.

Borkowski, et al. [1] conducted the numerical tests of impact of a steering angle of the Suzuki Swift car on the concrete road barrier. The paper shows the trajectories of movement and deformations of the vehicle corresponding to the collision angles of 10°, 20°, 30°, 40°. The numerical model of the vehicle was taken from the NCAC library. In another paper [2], the numerical modelling and simulations of TB11 and TB32 crash tests taking into account immobile or mobile segments of the concrete road barrier were developed. The results include the behaviour and deformation of the vehicles and the ASI index. The tests were performed using Suzuki Swift (TB11) and Dodge Neon (TB32) cars taken from the NCAC public library. The deformable couplers and fittings were modelled using four-node shell elements.

The paper [16] considers the selected extreme road barrier of the N2-W4-A class, with the B-type guide bar, on the horizontal, concave curve of a main road of accelerated motion, with an allowable radius in a road axis of 140-220 m. In order to ensure the adoption of the TB11 crash test, a composite-foam-rubber crash barrier, which was connected with the B guide bar with screw connections, using only free holes in the guide bar axis present at 2.00 m, was designed. Methodology of the numerical modelling and simulation of unmodified (a straight barrier) and modified (a curved barrier) TB11 crash test, without and with the crash barrier. Virtual TB11 crash tests were conducted in reference to the above four structural arrangement of the barrier. The Suzuki Swift vehicle model, appropriately amended, was taken from the public library of the National Crash Analysis Center, USA. The system LS-Dyna v971 was applied in the crash test simulations. It was shown that the barrier with a crash barrier in a horizontal, concave curve provides adoption of the crash test TB11.

This paper proposes a methodology of a TB51 virtual crash test on the example of the selected bridge barrier KTC 015 (KTC Polska Sp. z o.o., Bielsko Biała), using a simplified

coach model. The simulation results corresponding to the simplified model were compared with the simulation results for a quasi-accurate model and the experimental crash test results. In simulations of crash tests, the non-linear, explicit finite element code LS-Dyna v971 was used. The original names of the parameters and options of the LS-Dyna [12, 13] were applied.

2. Road protective barrier

For experimental and numerical tests, a KTC 015 extreme bridge protective barrier, offered on the market by the KTC Poland Sp. z o.o. company in Bielsko-Biała, shown in Figures 1, 2 [11] was chosen. The barrier consists of an A-type guide bar, absorbers (brackets) and the double-T posts attached to the base of the post with six ribs. Guide bar segments with a length of 4,320 mm are end-jointed using 8 screws. The connection of the guide bar with the bracket uses one screw and the connection of the bracket with the post – two screws. The screws are of the M16 diameter and the 5.8 class. The posts are fixed to the concrete bridge using 4 Hilti M24 chemical anchors in the 5.6 class. Table 1 gives the KTC 015 system's parameters.
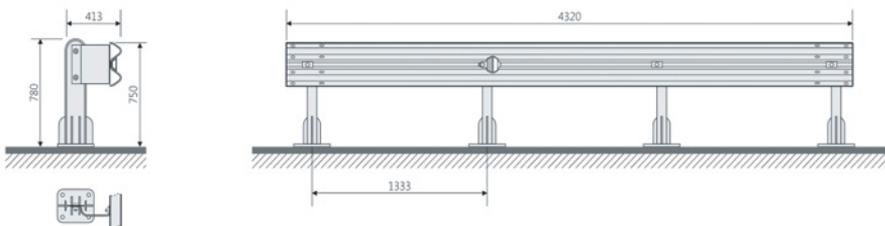

Fig. 1. KTC 015 system [11]

Fig. 2. Dimensions of the repeating fragment of the KTC 015 system [11]

Table 1. KTC 015 system's parameters [11]

Parameter name	Description/value
Barrier type	bridge, extreme
Restraint level	H2
Working width	W3
Vehicle intrusion class	VI5
Post spacing [m]	1.33
Tested system length [m]	60
Barrier height above terrain [m]	0.75

3. Numerical model of the KTC 015 system

The numerical model of the KTC 015 system with a length of 60 m, as shown in Figures 3, 4, was developed. The model consists of ~80,000 shell finite elements, with the QUAD4 and TRIA3 topologies in the ELFORM_2 formulation. The shell elements have 1 integration point on the surface and 5 on the thickness. Because of the use of elements of a limited number of integration points, hourglassing control according to the Flanagan-Belytschko procedure (IHQ = 4, QM = 0.03) was applied [18].

Components of the KTC 015 system were made of the S235JR steel. Yield strength Re = 340 MPa and tensile strength R_m = 440 MPa were received from strength tests. The MAT_024 material model was applied [6]. The model requires the introduction of actual stresses in a function of actual deformations. Based on the courses of engineering stresses in the function of engineering deformations, transformational [7] and extrapolation formulas (actual deformations are several times larger than the engineering ones) known from a tensile strength test, constants for the material model of the system component elements were set. The parameter responsible for the destruction (EPS efficient plastic deformations [6]) was set on the basis of numerical simulations of tensile stress of a sample until the destruction and it was chosen so that the sample breaks at engineering deformations resulting from experimental tests of samples' tensile stress.
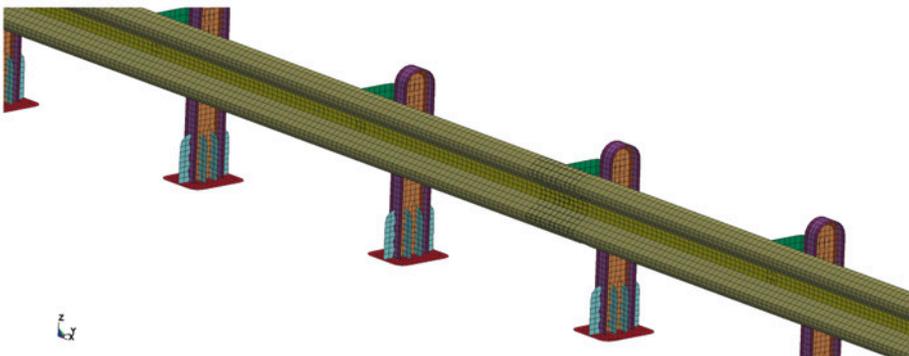

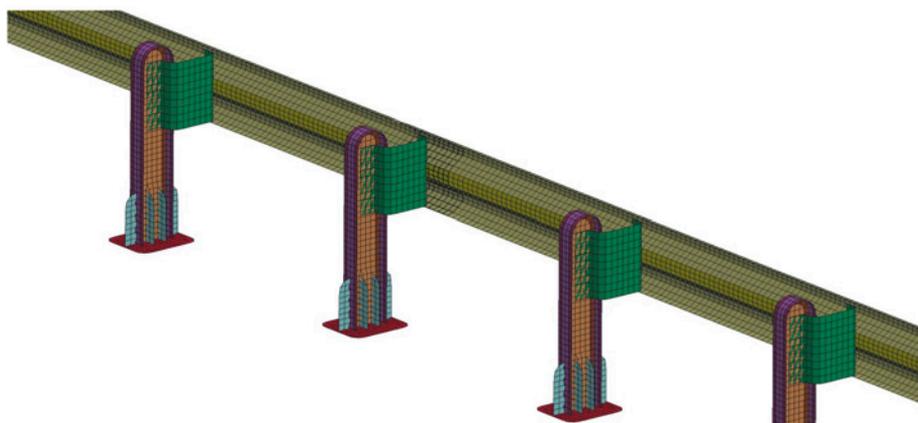Fig. 3. Front view of the numeric model of the KTC 015 barrier

Fig. 4. Back view of the numeric model of the KTC 015 barrier

Screw connections in protective road barriers are the one of the most important factors affecting the operation of the barrier and its functional parameters. That is why it is very important to model the joints, their rigidity and destruction parameters properly. This can be done with accurate or simplified modelling the joints. Due to the different scale of the numerical model of the barrier and a single joint, it was decided to model the connections in a simplified way. Due to the large number of joints in the KTC 015 system, rigidity properties and destruction parameters were set only for the joints destructed during the experimental test. These are the absorber-guide bar joints. The calculations were executed in accordance with the concept given in the paper [12]. For this purpose, a numerical 3D model was developed and simulation of stretching and shear of a single absorber-guide bar joint cut from the global model of the barrier (Fig. 5) was conducted.

In 3D modelling of the absorber-guide bar, the finite elements of the HEX8 and PENTA6 topologies, in the ELFORM_1 formulation, with hourglassing control according to the Flanagan-Belytschko procedure (IHQ = 4, QM = 0.03) [18] were applied. The cut guide bar fragment (yellow) was supported on the entire circumference by taking away all the degrees of easiness. The external surface of the folded absorber fragment (brown colour) underwent kinematic excitation at the right end, in the horizontal direction parallel to the plane of the system symmetry (Fig. 5a). Test conditions are similar to the case, in which the disconnection of the connection may occur at the moment of impact of the vehicle into the barrier. As a result, the rigidity properties and destruction parameters of the absorber-guide bar screw connection used in KTC 015 were received. Figs. 5b, c show the deformation in the selected time points until the destruction of the tested joint. Figure 6 shows the course of strength in the displacement function.

The material data of the M16 screws in the 5.8 class were taken from the standard [15]. The MAT_024 numerical model was applied. In order to determine the appropriate material constants, it was necessary to conduct preliminary numerical analyses of tensile stress

of the cylindrical sample with the diameter equal to the screw core. The material data (the value of the ETAN tangential module) and destruction parameter (efficient plastic deformations) were chosen so that the sample breaks at the engineering deformations and the forces resulting from the standard [15].
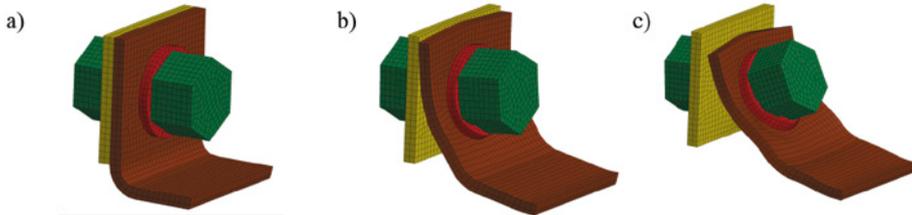

Fig. 5. Absorber-guide bar joint in subsequent load phases until breakage
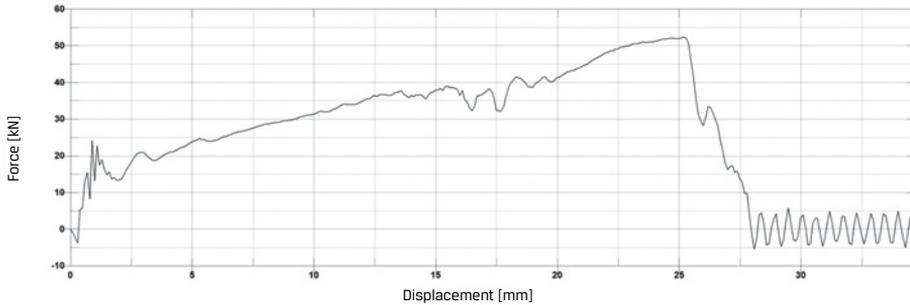

Fig. 6. Course of strength in the displacement function for the absorber-guide bar joint

The material of the other joints and anchors, which were not destroyed, were adopted as an elastic-plastic one with strengthening, without destruction. The modulus of elasticity E=210 GPa and tangential module ETAN=1 GPa were adopted, and the tensile strength was adopted from the standard [15]. For the screw of the 5.8 class, we have R_e = 420 MPa, and for the 5.6 anchors – tensile strength R_e = 300 MPa.

4. Experimental validation of numerical modelling

The KTC 015 system underwent a field test TB51 according to the standard [5]. This study is based on hitting the system with a coach with a mass of ~13,000 kg at an angle of 20°. The initial speed of the impact is 70 km/h. The quasi-accurate model of the coach was downloaded from the NCAC library, USA [10]. Although the model was consistent with the guidelines of the standard [5], multivariate, calibration, numerical analyses focused on the selection of appropriate stiffness of the front part of the coach were necessary. After the appropriate changes to the design of the front part of the vehicle, validation simulations were commenced.

The compatibility of the phenomenon course of a vehicle collision with the barrier and the received functional parameters of the barrier from the experimental and numerical test were tested. The simulation took into account the contact interaction with the friction between the vehicle and the barrier, the wheels and the surface and gravitational interaction. Kinetic friction coefficients corresponding to the Coulomb model are: vehicle-barrier: μ_k = 0.05, wheel-surface: μ_k = 0.5. Too low friction coefficients based on previous experiences and the fact that the guide bar, road and coach surfaces were covered with a layer of dust and sand were adopted.

Figure 7 shows the deformation of the real and virtual systems in selected time points. The footages were made available by KTC Polka Sp. z o.o. company of Bielsko Biała.
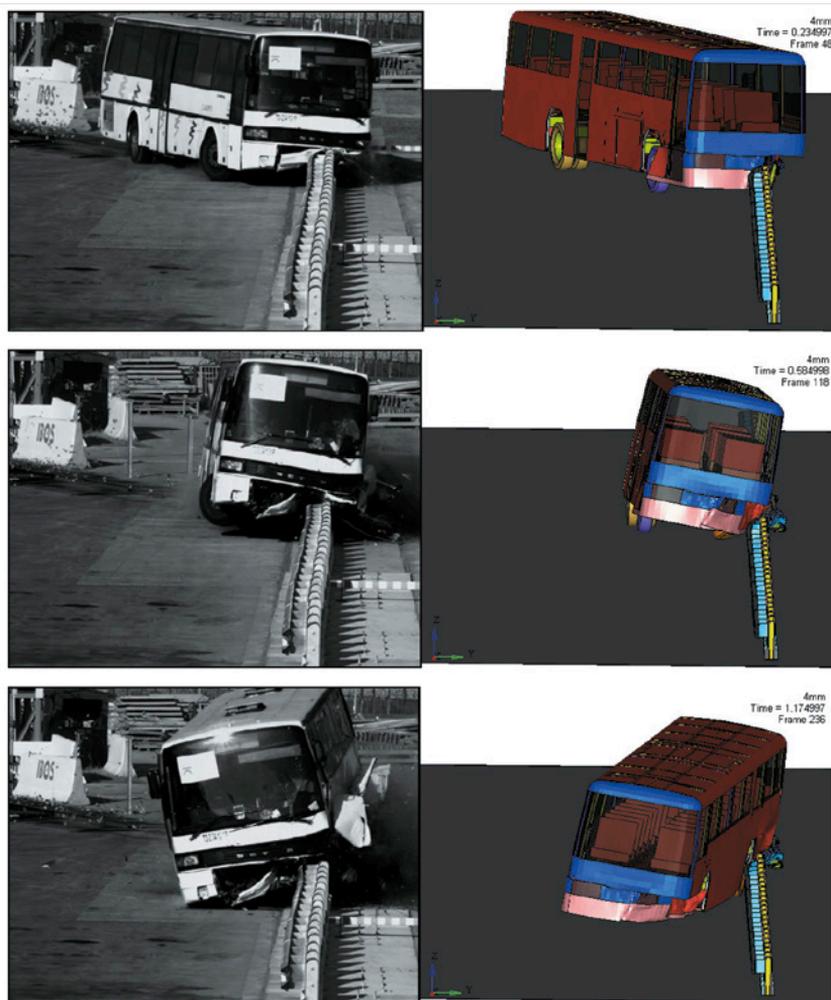

Fig. 7. Deformations of the vehicle-barrier system in selected time points

Table 2 summarised the functional parameter of the barrier in the experimental and numerical tests. The large discrepancy in the value of the standardised vehicle intrusion VIn results from the failure to take into account the wing mirrors in the numerical model. Assuming that the wing mirrors protrude 400 mm from the contour of the vehicle, the numeric result will be consistent with the experimental result.

Table 2. Functional parameters of the KTC 015 system received in the experiment and simulation

System parameter	Experiment	Simulation
Standardised dynamic deflection D_n [m]	0.85	0.78
Standardised working width W_n [m]	1.0	0.91
Standardised vehicle intrusion VI_n [m]	1.6	1.2 + wing mirrors
Static working width	0.86	0.86

After the experimental validation of the numerical modelling of hitting the quasi-accurate vehicle against the barrier, you can formulate the following conclusions:

1. The functional parameters of the systems do not only depend on the systems themselves, but also the properties of the vehicles involved in the incident. Without modification of a detailed numerical model of the vehicle, obtaining compliances with the functional parameters of the certification test is very difficult, and sometimes impossible. This is related to the differences in vehicles construction and their inertial properties. Depending on the placement of extra masses in the actual test, a different test result may be obtained.

2. Displacements of vehicles obtained numerically and experimentally are very similar in the initial phase of impact. Then, the phenomenon waveforms differ from each other because of different vehicles design and locking the guide bar in the vehicle during the experimental test.

3. The standardised functional parameters obtained numerically vary by up to 10% from those obtained experimentally.

4. The static working width obtained numerically practically does not differ from the one obtained experimentally.

Because of ever occurring design incompliances of the vehicle used in the experiment (different brand, different year of production, high risk of vehicle's running down) and the virtual vehicle of the NCAC library [10] as well as calibration problems resulting from high complexity of numerical models, the author proposes a simplified coach model for certifying numerical simulations of the modified systems.

5. Subject of tests

Bearing in mind that simulations with the simplified coach model are to demonstrate that the system modifications do not change the functional parameters of the barrier and are not of validation nature, the vehicle and the associated parameters (e.g. standardised vehicle intrusion VIn) are not critical. Therefore, the simplified vehicle should have as the simplest structure as possible. The influence of a suspension, wheel friction with the road surface, rotation around horizontal central axes of the vehicle were abandoned and the crash box was simplified to the maximum. The aim is to reduce the simulation and to make the vehicle model calibration possible. Such an approach will also help certification bodies because of the simplification and standardisation of vehicles used in the simulations of hitting the barrier. The less variables, the easier the phenomenon analysis is. A simplified coach model shown in Figure 8 was proposed.
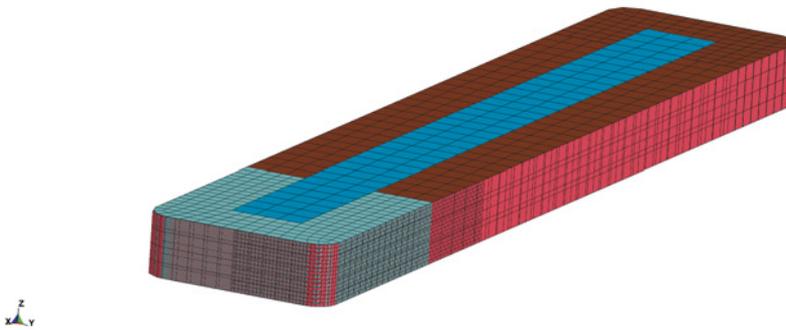

Fig. 8. Simplified coach model. General view

The simplified vehicle is a prism with rounded, vertical edges, whose external dimensions are consistent with the actual vehicle (Fig. 9). Rounding radii are 300 mm. The vehicle height depends on the height of the tested system; in the tested case, it is 800 mm. The height above ground level is equal to the height above the ground level of the vehicle body from the NCAC base (Fig. 10).
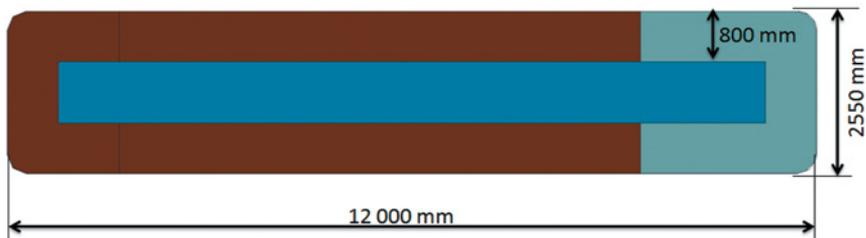

Fig. 9. External dimensions of a simplified coach model
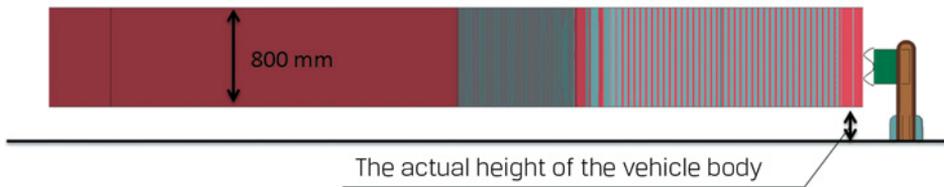
800 mm

The actual height of the vehicle body

Fig. 10. Height of a simplified coach model above the surface level

The central part of the vehicle is a non-deformable core with mass-inertial properties corresponding to the actual vehicle. These properties do not result directly from the geometry and density of the core, but from measurements of the inertia moments and the location of the centre of gravity of the coach model from the NCAC base [10] and were given to the core via the *PART_INERTIA card [6]. Such an approach greatly simplifies the potential changes of the inertia moments in the case of the creation of other vehicles and calibration simulations. As it is known, the distributions of additional masses in the vehicle has a real influence on the phenomenon course, hence the inertia moment with respect to the central vertical axis is an additional variable that needs to be taken into account in the simulation.

The core is surrounded with a deformable material of a foamed material properties. The foamed material was divided into two zones of different stiffness – into the front part (blue) and the other one (brown) (Fig. 9). Such a division is necessary because sometimes there is a secondary impact with the barrier with a rear part of the vehicle, the stiffness of which is usually different from the front one. By changing the stiffness of the deformable material and the said inertia moments, the vehicle is calibrated in order to obtain the functional parameters consistent with those obtained in an experimental crash test. The deformable/foamed material is covered with a metal sheet of a thickness resulting from the thickness of the body's metal sheet in the actual vehicle. In the case of the coach, the body's metal sheet thickness is 2 mm.

The replacement vehicle core can move only in longitudinal and transverse directions. The ability of movement in the vertical direction was deliberately blocked in order to reduce the number of variables affecting the phenomenon to a minimum. Blocking the ability of movement of the vehicle in the vertical direction and, additionally, the rotation in relation to the horizontal central axes of the vehicle limits the number of inertia moments to one in relation to the vertical axis. The angle of vehicle impact is 20° and the initial speed is 70 km/h. The simulation took into account the contact interaction with the friction of the vehicle with the barrier and gravitational interaction.

The MAT_026 model [6] was used to describe the foamed material surrounding the non-deformable core. Table 3 shows the material constants of the foamed material of the front zone of the vehicle, and Figures 11, 12 show the required curves [14]. By changing the scale coefficient of CURVE1 and CURVE2, it was possible to change the rigidity of the foamed

material and, thus, the model calibration. The material constants of the foamed material from the remaining part of the vehicle differ only in CURVE1 and CURVE2. These curves were scaled with the coefficient of 10.

Table 3. Material constants of the foamed material [14]

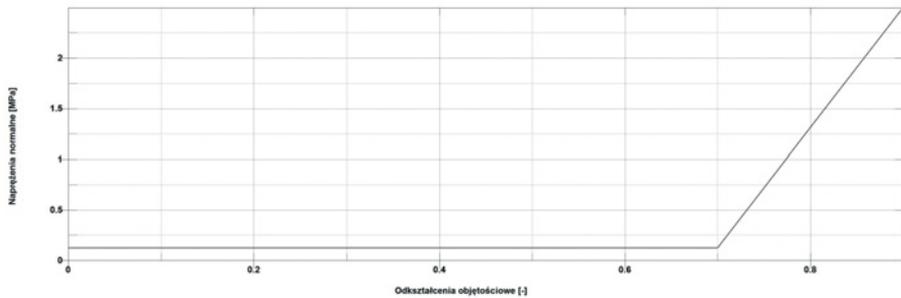| Parameter in LS-DYNA	Value	Unit
RO	100	kg/m^3
E	1000	MPa
PR	0.3	-
SIGY	50	MPa
LCA, LCB, LCC	CURVE1	MPa
LCS, LCBC, LCCA, LCAC	CURVE2	MPa
EAAU, EBBU, ECCU	5	MPa
GABU, GBCU, GCAU	2	MPa

Fig. 11 CURVE1. Normal stresses in a function of dilatational strains
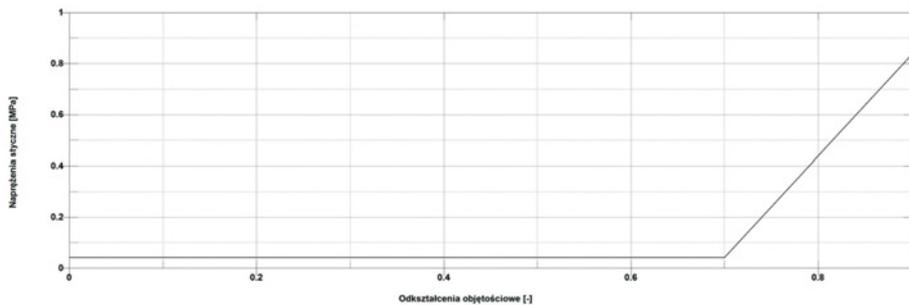

Fig.12. CURVE2. Shear stresses in a function of dilatational strains

6. Results of simulation and their analysis

The state of virtual displacement of the virtual simplified and quasi-accurate vehicles was compared. Figure 13 presents the results in selected time points. Figure 14 shows displacements of the barrier in a direction transverse to the axis of the barrier for an impact with the quasi-accurate and simplified vehicle. Table 4 compared the functional parameter of the barrier depending on the vehicle.
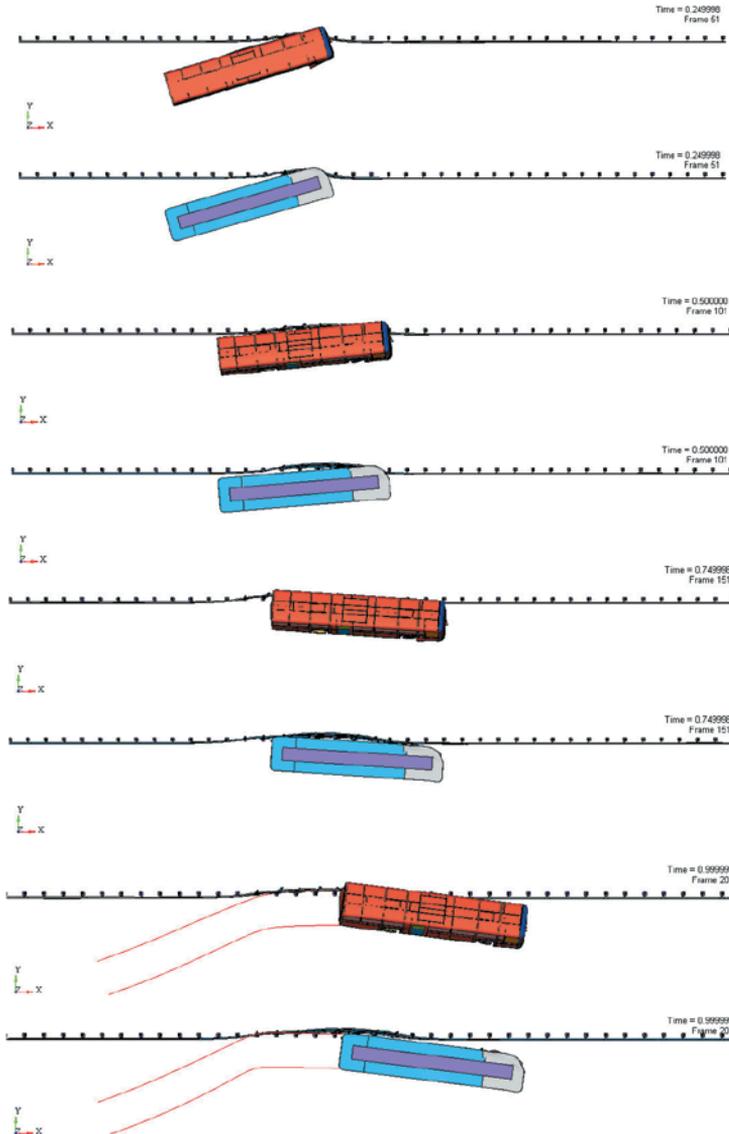

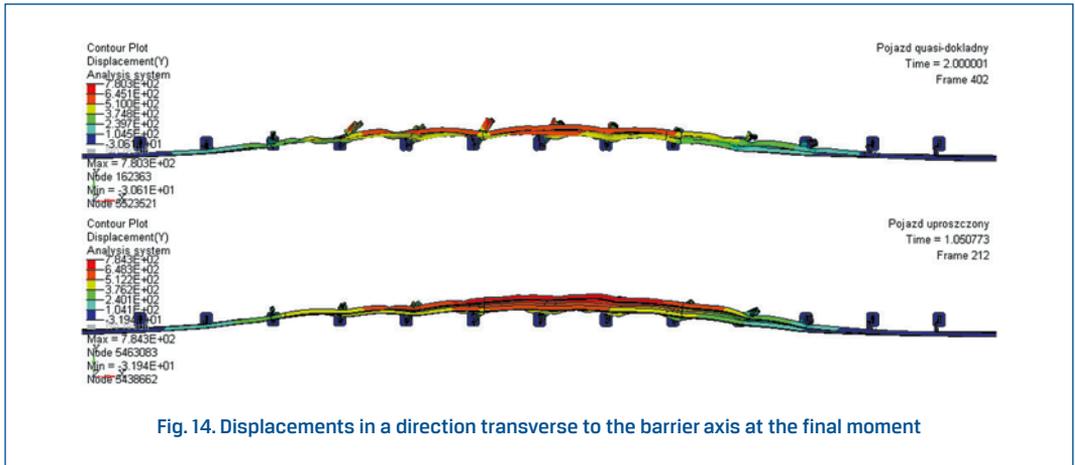Fig. 13. Displacements of vehicles in selected time points

Fig. 14. Displacements in a direction transverse to the barrier axis at the final moment

Table 4. Functional parameters

System parameter	Experimental vehicle	Quasi-accurate vehicle	Simplified vehicle
Standardised dynamic deflection D_n [m]	0.85	0.78	0.79
Standardised working width W_n [m]	1.0	0.91	0.87
Standardised vehicle intrusion VI_n [m]	1.6	1.2 + wing mirrors	-
Static working width	0.86	0.86	0.86

After the simulation of the impact with the simplified and quasi-accurate vehicle against the barrier, you can formulate the following conclusions:

1. The displacements of the vehicles in the numerical tests are similar. Subsequent phases of the impact are compatible.

2. Functional parameters are similar in both cases.

3. The displacements of the system at the end of the phenomenon are very similar in terms of quality and quantity.

4. The calibration of the simplified vehicle in the first attempt comes down to a change in the scale coefficient of CURVE1 and CURVE2. As a result, the calibration process is simplified. If the change of the scale coefficient does not produce sufficient results, you can slightly modify the inertia properties of the simplified model.

5. Thanks to the maximum simplification of the replacement vehicle, computing time of the system decreases 4 times.

6. The replacement vehicle is well conditioned, and the results are not as sensitive to changing parameters as in the case of the quasi-accurate model. There is no, among

others, influence of suspension features, the complicated structure of the vehicle and the material properties of hundreds of vehicle components.

Acknowledgements

The full text of the Article is available in Polish online on the website
http://archiwummotoryzacji.pl.

Tekst artykułu w polskiej wersji językowej dostępny jest na stronie
http://archiwummotoryzacji.pl.

References

[1]   Borkowski W, Hryciów Z, Rybak P, Wysocki J. Testing the results of a passenger vehicle collision with a rigid barrier. J. KONES Powertrain and Transport. 2010; 17(1).

[2]   Borkowski W, Hryciów Z, Rybak P, Wysocki J. Numerical simulation of the standard TB11 and TB32 tests for a concrete safety barrier. J. KONES Powertrain and Transport. 2010; 17(4).

[3]   Dziewulski P. Badanie wybranych struktur do poprawy energochłonności drogowych barier ochronnych. [Test of selected designs to improve the energy consumption of road protective barriers]. Doctoral thesis, Faculty of Mechanical Engineering, Military University of Technology. Warsaw, 2010.

[4]   EN 1317-1:2010. Road restraint systems – Part 1: Terminology and general criteria for test methods.

[5]   EN 1317-2:2010. Road restraint systems – Part 2: Performance classes, impact tests acceptance criteria and test methods for safety barriers including vehicle parapets.

[6]   Hallquist J O. LS-DYNA Keyword User's Manual. Livermore Sofware Technology Corporation; 2007.

[7]   Hallquist J O. LS-DYNA Theory Manual. Livermore Sofware Technology Corporation; 2006 USA.

[8]   Kiczko A, Niezgoda T, Nowak J, Dziewulski P. Numerical implementation of car impact into the modified road barrier. J. KONES Powertrain and Transport. 2010; 17(3): 189-196.

[9]   Ren Z, Vesenjak M. Computational and Experimental Crash Analysis of the Road Safety Barrier. Engineering Failure Analysis. 2005; 12: 963-973.

[10] Vehicle Models, National Crash Analysis Center, USA. Available from: http://www.ncac.gwu.edu/vml/models.html.

[11] Offer of road and bridge protection barriers. Available from: http://www.ktcpolska.eu/.

[12] Nycz D. Modelowanie i badania numeryczne testów zderzeniowych bariery klasy N2-W4-A na łukach dróg. [Modelling and numerical studies of crash tests of an N2-W4-A class barrier on road curves.] 2015. Doctoral monograph, Wydawnictwo WAT, Warszawa 2015.

[13] http://www.dynasupport.com/howtos/material/from-engineering-to-true-strain-true-stress.

[14] Klasztorny M, Małachowski J, Dziewulski P, Nycz D, Gotowicki P. Experimental investigations and modelling of alporas aluminium foam. Modelling in Engineering. 2012; 12(43): 97-112.

[15] PN-EN ISO 898-1:2013. Mechanical properties of fasteners made of carbon steel and alloy steel – Part 1: Bolts, screws and studs with specified property classes – Coarse thread and fine pitch thread.

[16] Klasztorny M, Nycz D B, Romanowski R K. Rubber/Foam/Composite Overlay on Guide B of Barrier Located on Road bend. The Archives of Automotive Engineering – Archiwum Motoryzacji. 2015; 69(3): 65-86.

[17] PN-EN 1317-5+A2:2012. Road restraint systems – Part 5: Product requirements and evaluation of conformity for vehicle restraint systems.

[18] Bala S, Day J. General guidelines for crash analysis in LS-DYNA, Livermore Sofware Technology Corporation, USA.